Mode I Fatigue Growth Analysis of a Sickle-shaped Surface Crack in a Cylindrical Bar

Andrea Carpinteri, Roberto Brighenti, Matteo Boni, Sabrina Vantadori, Danilo Viappiani

Department of Civil and Environmental Engineering & Architecture, University of Parma - Viale G.P. Usberti, 181/A – 43100 Parma – Italy
E-mail: andrea.carpinteri@unipr.it ; sabrina.vantadori@unipr.it

ABSTRACT. *The fatigue growth of a sickle-shaped surface crack in a metallic round bar under bending loading is examined. The flaw, located in a plane perpendicular to the longitudinal axis of the bar, is assumed to present an elliptical-arc shape during the whole propagation and, therefore, can be defined by the crack depth at the most internal point on the defect front, and the aspect ratio of the above ellipse. Linear elastic fracture mechanics concepts are used to calculate the Stress-Intensity Factor (SIF) along the crack front, by employing a 20-node isoparametric finite element model with quarter-point wedge finite elements arranged near the defect. The SIF values are computed using the one-quarter point displacement method and assuming the plane strain condition along the crack front. The numerical results obtained are compared with experimental data available in the literature. Then, a procedure based on the Paris-Erdogan law is applied in order to simulate the crack growth under cyclic bending. Fatigue analysis results are presented in terms of crack paths for some initial flaw geometrical configurations being examined.*

INTRODUCTION

Round bars, such as bolts, screws and reinforcements, are used in important engineering applications. Notches or material discontinuities can cause crack initiation and, due to cyclic loading, fatigue crack propagation can occur.

Since the stress field near the crack front is represented by the Stress-Intensity Factor (SIF), many studies have been performed to determine the SIF variation along the front of surface cracks in cylindrical bars. According to experimental observations, such flaws often present an almond shape [1-11], but sickle-shaped cracks are also frequent in round bars, even if only a few studies have been carried out to derive the SIF values for the latter case [12,13].

In the present paper, a sickle-shaped surface crack in a round bar subjected to bending moment M_X is considered (Fig. 1). The geometrical configuration of the flaw is defined by means of two parameters: the relative crack depth $\xi = a/D$ at point A on the defect front, and the crack aspect ratio $\alpha = a_{el}/b_{el}$ (Fig. 1b). The parameter ξ is made to vary from 0.1 to 0.8, whereas α ranges from -1.2 to 0.0. Note that $\alpha < 0.0$ means that the ellipse describing the crack front has an upward concavity in the 2D-coordinate

system XY in Fig. 1b (sickle shape); $\alpha > 0.0$ represents a crack front with a downward concavity (almond shape); finally, $\alpha = 0.0$ represents a straight-fronted crack.

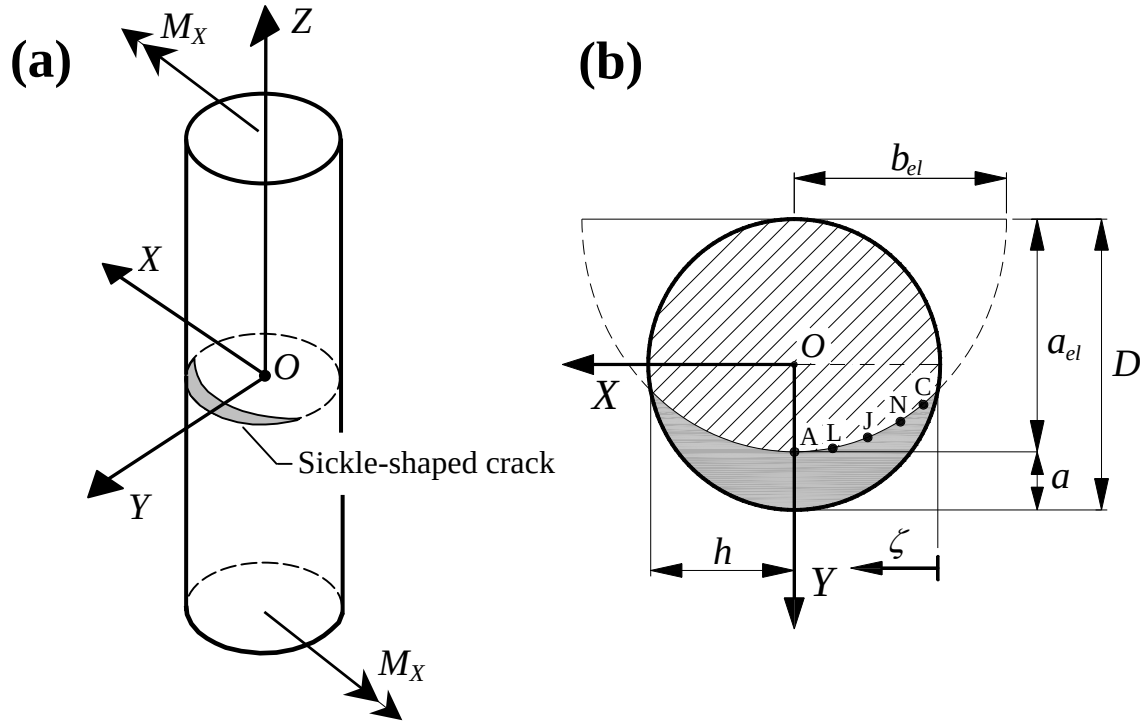

Figure 1. Round bar with a sickle-shaped surface crack ($\alpha < 0.0$): (a) loading condition (bending moment M_X); (b) geometrical parameters.

Stress-Intensity Factor values along the crack front are computed through a three-dimensional finite element analysis. The numerical results obtained are compared with those experimentally determined by Radebe [14], and a satisfactory agreement is found.

Then, fatigue growth of sickle-shaped surface cracks is numerically analysed for round bars subjected to constant amplitude cyclic bending M_X . During last decades, extensive research work has been carried out in order to examine the fatigue behaviour of round bars with an almond-shaped crack [8,15-18], but only a few authors have simulated the fatigue crack shape evolution starting from an initial defect with an irregular or sickle shape [19,20].

Fatigue propagation of a crack with an initial sickle shape is hereafter analysed by means of a two-parameter model [18] based on the Paris-Erdogan law [21]. The surface flaw is assumed to present an elliptical-arc shape during the whole propagation, as some authors have analytically and experimentally deduced [4,22]. Predictions of the crack front evolutions are presented for six initial defects. It can be remarked that the sickle-shaped crack front tends to gradually become flat and then changes its concavity, that is, the crack aspect ratio α goes from negative to positive values by increasing the relative crack depth ξ.

NUMERICAL EVALUATION OF THE STRESS INTENSITY FACTOR

Stress-Intensity Factor values for bending loading M_X are calculated by applying the finite element method and linear elastic fracture mechanics (LEFM). Because of symmetry, only a quarter of the round bar has been modelled, using 20-node isoparametric finite elements and one ring of quarter-point wedge finite elements in the vicinity of the flaw front (Fig. 2). The SIF is computed at points A, L, J, N, C (Fig. 1b) using the one-quarter point displacement method, and assuming the plane strain condition along the whole crack front. Each point on the crack front is identified by its dimensionless coordinate $\zeta^* = \zeta / h$ (Fig. 1b).

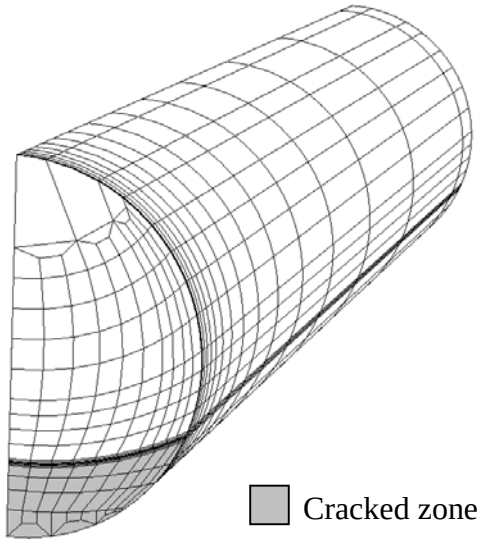

Figure 2. Three-dimensional finite element mesh.

The dimensionless SIF under Mode I is computed as follows:

$$K^*_{I,M_X} = \frac{K_{I,M_X}}{\sigma_{M_X}\sqrt{\pi a}} \tag{1a}$$

where

$$K_{I,M_X} = \text{SIF for bending;} \quad \sigma_{M_X} = \frac{32\,M_X}{\pi D^3}\ ; \quad a = \text{crack depth at point A} \tag{1b}$$

As far as the numerical simulation of the crack growth is concerned, the most significant zones along the crack front are the central zone (point A) and the external zone (point C). Therefore, the SIFs for such two points are plotted in Fig. 3 against the relative crack depth ξ, for α equal to -1.2, -1.0, -0.8, -0.6, -0.4, -0.2, 0.0.

The following remarks can be made:

- Each curve related to point A (Fig. 3a) increases by increasing the parameter ξ. For a given value of the relative crack depth, the value of K^*_{I,M_X} increases by decreasing the crack aspect ratio α;
- The curves related to point C (Fig. 3b) either increase or decrease by increasing the parameter ξ. For a given value of the relative crack depth, the value of K^*_{I,M_X} increases by increasing the crack aspect ratio α.

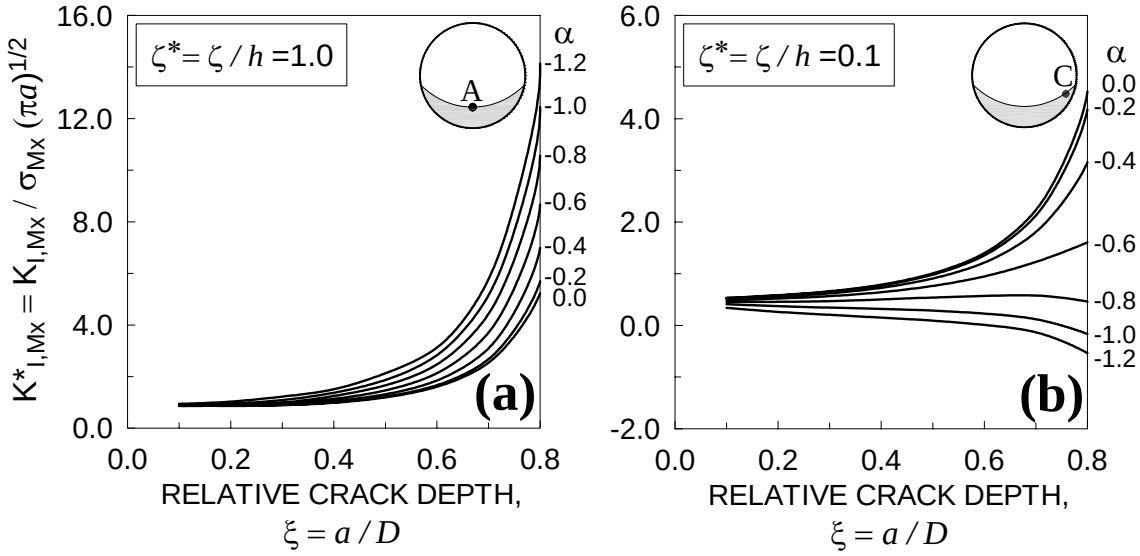

Figure 3. Dimensionless SIF K^*_{I,M_X} against relative crack depth ξ, for different values of the crack aspect ratio α: (a) point A; (b) point C.

In Figure 4, some numerical results (SIF K^*_{I,M_X} at point A) are compared with those experimentally determined by Radebe [14]. The agreement is quite satisfactory, even if the Radebe's SIF values are slightly lower than the numerical results. The scatter could be due to the following reasons:

- The values of the parameters α and ξ experimentally measured by Radebe are related to crack fronts which are not exactly elliptical arcs;
- In some of the experimental cases, the crack shape is not exactly symmetric with respect to the *Y* axis (Fig. 1b).

As can be observed in Fig. 4, both numerical and experimental SIFs are well fitted by second order polynomials (dashed lines).

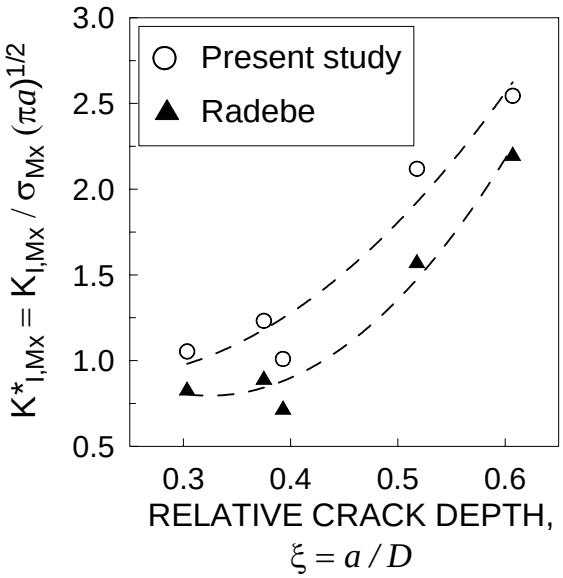

Figure 4. Dimensionless SIF, K^*_{I,M_X} , at point A against relative crack depth ξ : numerical results (present study) and experimental data (Radebe [14]).

FATIGUE CRACK GROWTH SIMULATION

The SIFs previously calculated are employed to study the fatigue propagation of a sickle-shaped crack under cyclic bending loading. The Paris-Erdogan law [21] is applied to obtain the local crack depth increments (perpendicular to the crack front) at point A and point C (Fig. 1b):

$$da / dN = A\left(\Delta K_I\right)^m \tag{2}$$

where da / dN is the crack growth rate, and A and m are constants of the material. The crack front is assumed to have an elliptical-arc shape during the whole fatigue propagation, as several authors have analytically and experimentally deduced [4,22]. The cyclic bending loading presents a constant amplitude stress range $\Delta\sigma_{M_X}$ = 100 MPa and loading ratio equal to 0.0, whereas the material constants are assumed to be m = 2 and $A = 1.64 \times 10^{-10}$ (with da / dN in mm cycle^{-1} and ΔK_I in N mm$^{-3/2}$). Details of the numerical procedure used to simulate the crack propagation can be found in Ref.[18].

Figure 5 shows the crack propagation paths (i.e. crack aspect ratio against relative crack depth) for six initial crack configurations (see from No.1 to No.6). The values α_0 and ξ_0 define the initial flaw geometry.

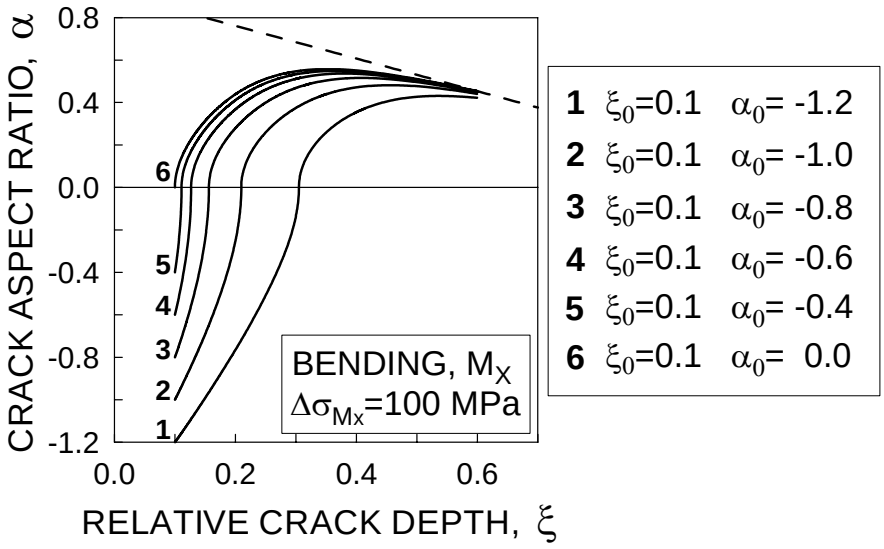

Figure 5. Crack aspect ratio against relative crack depth during fatigue crack growth.

As far as Figure 5 is concerned, it can be remarked that:

- For negative values of α_0 (sickle-shaped cracks), the crack growth path slope for ξ = 0.1 increases by increasing the initial crack aspect ratio α_0 ; for example, see curve No.1 (α_0= -1.2) compared with curve No.2 (α_0=-1.0);
- For the curves Nos 1, 2, 3, 4, 5, the crack front shape changes from a sickle shape (α < 0.0) to an almond shape (α > 0.0) in correspondence to a given value of ξ. Such a particular value of ξ increases by decreasing the initial crack parameter α_0;
- All propagation paths in Figure 5 tend to converge to an inclined asymptote (see dashed line).

For two initial surface cracks considered in Fig. 5 (sickle shape related to case No.1 and straight-fronted shape related to case No.6), the fatigue crack front evolution is shown in Fig. 6a and Fig. 6b, respectively. The initial cracked surfaces are displayed in grey in Fig. 6. The crack growth stages are plotted for ξ from 0.1 to 0.6, with relative crack depth increments equal to 0.05. The following remarks can be made:

- Crack No.1 grows evolving from a sickle shape (α < 0.0) to an almond shape (α > 0.0). The sign of α changes in correspondence to ξ equal to about 0.3;
- After a few crack growth steps, the crack profiles for the two cases examined (No.1 and No.6) are quite similar even if the corresponding initial crack configurations are quite different from each other.

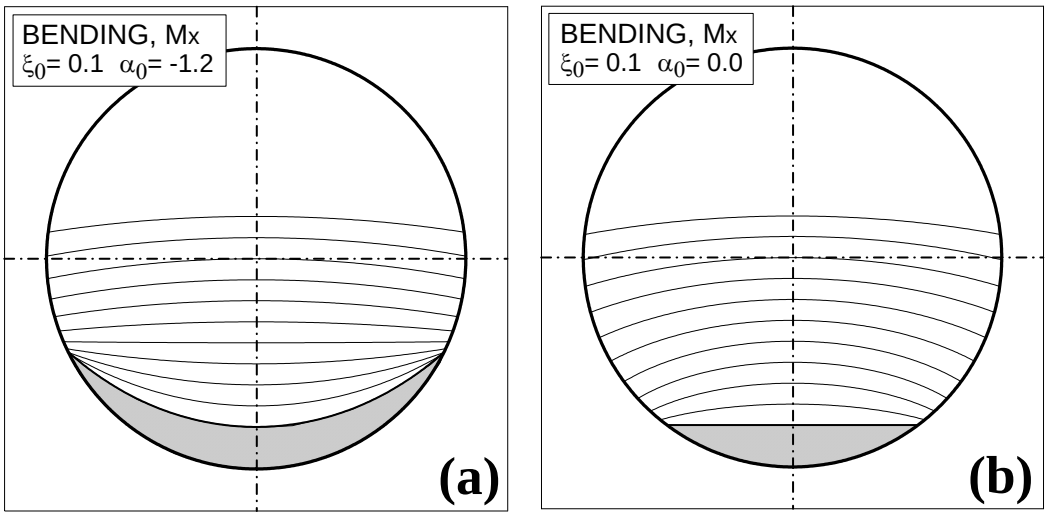

Figure 6. Predicted fatigue crack shape evolution for: (a) crack No. 1 (ξ_0=0.1, α_0=-1.2); (b) crack No. 6 (ξ_0=0.1, α_0= 0.0).

CONCLUSIONS

The mechanical behaviour of a round bar with a sickle-shaped crack under bending loading has been examined.

Firstly, the Stress-Intensity Factor along the crack front has been determined by using the finite element method together with fracture mechanics concepts. The results obtained have shown that, for the crack configurations examined, the most critical parts along the crack front are the internal point A and the near-surface point C. The SIF values deduced numerically have been compared with some experimental results available in the literature, and a satisfactory agreement has been found.

Then, the fatigue crack growth has been analysed through a procedure based on the Paris-Erdogan law. It has been shown that:

- The initially sickle-shaped cracks examined change the crack front shape from a sickle shape ($\alpha < 0.0$) to an almond shape ($\alpha > 0.0$) in correspondence to a given value of the relative crack depth;
- The crack propagation paths tend to converge to an inclined asymptote in the diagram of the flaw aspect ratio against the relative crack depth.

ACKNOWLEDGEMENTS

The authors gratefully acknowledge the research support for this work provided by the Italian Ministry for University and Technological and Scientific Research (MIUR).

REFERENCES

1. Daoud, O.E.K., Cartwright, D.J., Carney, M. (1978) *J. of Strain Analysis* **13**, 83-89.
2. Pook, L.P. (1983). *The Role of Crack Growth in Metal Fatigue*, Metals Society, London.
3. Raju, I.S., Newman, J.C. (1986). In: *Fract. Mech. 17th Volume*, pp.789-805, ASTM STP 905.
4. Caspers, M., Mattheck, C. (1987) *Fatigue Fract. Engng Mater. Struct.* **9**, 329-341.
5. Carpinteri, A. (1991) *Engng Fract. Mech.* **38**, 327-334.
6. Carpinteri, A. (1992) *Engng Fract. Mech.* **42**, 1035-1040.
7. Levan, A., Royer, J. (1993) *Int. J. Fracture* **61**, 71-99.
8. Carpinteri, A. (Ed.) (1994). *Handbook of Fatigue Crack Propagation in Metallic Structures*, Elsevier Science BV, Amsterdam.
9. Carpinteri, A., Brighenti, R. (1996) *Int. J. Fatigue* **18**, 33-39.
10. Pook, L.P. (2002) *Crack Paths*. WIT Press, Southampton.
11. Carpinteri, A., Brighenti, R., Vantadori, S. (2006) *Int. J. Fatigue*, **28**, 251-260.
12. Makhutov, M., Zatsarinny, V., Kagan, V. (1981). In: *Advances in Fracture Research*, pp.605-612, Francois, D. (Ed.), Pergamon Press, Oxford.
13. Mattheck, C., Morawietz, P., Munz, D. (1985) *Int. J. Fatigue*, **7**, 45-47.
14. Radebe, D.B. (2000). Undergraduate Thesis, University of Cape of Town, South Africa.
15. Lorentzen, T.K., Kjaer, N.E., Henriksen, T. (1986) *Engng Fract. Mech.* **23**, 1005-1014.
16. Caspers, M., Mattheck, C., Munz, D. (1987). In: *Surface-crack Growth: Models, Experiments, and Structures*, pp.365-389, ASTM STP 1060.
17. Sih, Y.-S., Chen, J.J. (1997) *Int. J. Fatigue* **19**, 477-485.
18. Carpinteri, A. (1993) *Int. J. Fatigue* **15**, 21-26.
19. Lin, X.B., Smith, R.A. (1998) *Int. J. Mech. Sci.* **40**, 405-419.
20. Lin, X.B., Smith, R.A. (1999) *Int. J. Fatigue* **19**, 461-469.
21. Paris, P.C., Erdogan, F. (1963) *J. Basic Eng Trans.*, ASME **85D,** 528-534.
22. Forman, R.G., Shivakumar, V. (1986) *Fract. Mech.* **30**, 59-74.